Annual Methodological Archive Research Review
http://amresearchreview.com/index.php/Journal/about
Volume 4, Issue 3 (2026)

Online ISSN 3007-3197
Print ISSN 3007-3189
http://amresearchreview.com/index.php/Journal/about

A Positivity-Preserving Finite Volume KFVS Scheme for Shallow Water Equations with Porosity and Non-Conservative Terms

Muhammad Azam*

Department of Mathematics, COMSATS University Islamabad, Pakistan.

Corresponding Author Email: muhammadazamjoyo01@gmail.com

Imran Munir

Department of Mathematics, COMSATS University, Islamabad, Pakistan.

Email: ravianbhattissg@gmail.com

ABSTRACT

Shallow water equations with porosity have recently been proposed to simulate flood dynamics in urban areas, where the water occupies only a fraction of the total surface area because of buildings and other obstacles. The governing equations form a system of non-linear, non-conservative partial differential equations that does not admit analytical solutions, and their numerical approximation is challenging because of the non-conservative terms, discontinuous porosity, complex bottom topography and the presence of dry zones. In this work, we develop a high-resolution finite volume method for the one-dimensional shallow water equations with porosity based on the Kinetic Flux-Vector Splitting (KFVS) scheme. The scheme splits the flux vector in an upwind-biased manner using a local Maxwellian distribution, so that no Riemann solver or entropy correction is required. The bed-slope and porosity source terms are discretized in a way that preserves the lake-at-rest steady state, and the resulting scheme is well balanced, and the numerical results indicate that the positivity of the water height is preserved. Second-order accuracy in space is obtained by a MUSCL-type piecewise-linear reconstruction with the minmod limiter, and second-order accuracy in time is achieved with a TVD Runge–Kutta method. To assess the accuracy and robustness of the proposed scheme, the numerical results are compared with those of the non-oscillatory central scheme of Nessyahu and Tadmor on four one-dimensional test problems: a dam-break problem over a bed step, a lake-at-rest steady-state problem, dam-break problems with discontinuous porosity, and a dry-bed dam-break problem. The results show that the KFVS scheme captures rarefaction waves, shocks and stationary discontinuities accurately, preserves steady states and handles

Annual Methodological Archive Research Review
http://amresearchreview.com/index.php/Journal/about
Volume 4, Issue 3 (2026)

Online ISSN 3007-3197
Print ISSN 3007-3189
http://amresearchreview.com/index.php/Journal/about

dry zones without special treatment. It also resolves sharp discontinuities somewhat better than the central scheme.

Keywords: Shallow water equations; Porosity; Non-conservative terms; Kinetic flux-vector splitting; Well-balanced scheme; Positivity-preserving; Central scheme; Urban flood modeling.

Introduction

In this research article, we discuss the motivation and importance of the present work. It provides an introduction to the shallow water equations and their importance in general, and to the shallow water flow equations with porosity in particular. Analytical solutions do not exist for the model equations. Therefore, we seek to obtain solutions using numerical methods.

1.1 Background and Motivation

Shallow water flow is a type of flow in which the vertical length scale is much smaller than the horizontal length scale; in other words, the longitudinal length is larger than the vertical length. The shallow water equations (SWEs) are mainly used to model the flow of water in rivers, lakes and coastal regions. Thus, they provide a basis for modeling a variety of problems related to the environment and coastal engineering. The shallow water equations were initially developed by A. J. C. de Saint-Venant [1]. Later, these model equations were further investigated by numerous authors, with extensions to one and two dimensions and generalizations to flows over more complex bottom topography [2, 3]. Recently, some authors have developed SWEs with porosity to model flood simulations in urban areas [4]. The addition of porosity to the model equations accounts for the fact that the area occupied by water is only a fraction of the total surface area [5].

A major challenge in solving SWEs numerically is to preserve the non-trivial equilibrium that arises due to the non-conservative terms. To address this, several authors have proposed different numerical techniques for the solution of SWEs with porosity. For example, upwind-type schemes were applied to the model equations with source terms at the boundary, see [6, 7, 8]. A Roe solver for the 2D Euler system of equations with porosity was implemented by the authors of [9]. A HLLC (Harten–Lax–van Leer contact) modified Riemann solver for the 2D SWEs with porosity is discussed in [10]. A finite volume method was successfully applied to the porosity-dependent SWEs on an unstructured mesh in [11]. The Rusanov method for SWEs with porosity was analyzed and studied for the spatial discretization by the authors of [12, 13]. The author of [14] implemented a finite volume method for SWEs with porosity. The purpose of the current work is to apply a robust algorithm.

The shallow water equations are a set of hyperbolic partial differential equations that

Annual Methodological Archive Research Review
http://amresearchreview.com/index.php/Journal/about
Volume 4, Issue 3 (2026)

Online ISSN 3007-3197
Print ISSN 3007-3189
http://amresearchreview.com/index.php/Journal/about

describe the motion of a fluid under a pressure surface, often, but not always, a free surface. Hyperbolic partial differential equations can contain shocks, rarefaction waves, etc.; a shock represents a discontinuity at which more than one solution value exists at a single point. The one-dimensional shallow water equations are also referred to as the Saint-Venant equations.

Multiphase shallow flows are important in many natural phenomena and industrial applications, ranging from power generation to the food and drink industry, oil and gas pipelines, chemical engineering and mining. A single-phase flow involves only one phase of matter (liquid, gas or solid), and typical hydrodynamic simulations focus on the motion of a single homogeneous phase, for example water, air or steam. If a liquid and a gas flow together in certain essential regions of a flow system, the problem has to be treated as a two-phase flow. A two-phase shallow flow model consists of volume and energy equations for the solid and liquid phases, combined with conservative and non-conservative terms of balance.

The shallow water equations have been used in many applications, such as river flow, reservoir break and open-channel flow. The model equations with porosity were recently proposed to model floods in urban areas. These equations cannot be solved analytically, and their numerical solution is a challenging task due to the presence of non-conservative terms. Because of the complexity of constructing suitable wave structures, finding an analytical solution is difficult, so we look for a numerical scheme that can solve such models accurately. Since a numerical scheme can introduce errors, it must be accurate, and the accuracy generally improves when a sufficiently fine mesh is used.

1.2 Literature Review

Porosity is basically the empty space in a material. Variations in the bed properties cause variations in the results, and porosity also affects the graphical results. Different authors have worked on shallow water problems with porosity. For example, in one dimension, Savage and Hunter obtained reasonably good results, after which some authors extended this work to the next level, such as two-phase shallow water flow involving porosity. The study of fluid behavior is always challenging, because the bottom may be non-flat, porous or sometimes smooth, and all these factors strongly affect the porosity. Therefore, we use an appropriate numerical scheme that gives the best possible result. As is known from the literature, it is not possible to find an analytical solution of the shallow water equations with porosity. The conserved form of the shallow water equations involves a source term due to the bottom topography, and the porosity must also be included so that the solution is represented accurately.

Pelanti and co-workers [7] worked on the proposed shallow water model and

Annual Methodological Archive Research Review
http://amresearchreview.com/index.php/Journal/about
Volume 4, Issue 3 (2026)

Online ISSN 3007-3197
Print ISSN 3007-3189
http://amresearchreview.com/index.php/Journal/about

showed that it has a hyperbolic character. In hyperbolic systems, shocks can occur, which means that the solution may be discontinuous at a given point. Keeping this basic knowledge of hyperbolic systems in mind, researchers moved to the next stage, which is the two-phase shallow water equations.

1.3 Numerical Challenges

When solving numerical problems, several issues arise that must be kept in mind. For the development of an appropriate, effective, and result-oriented scheme, the following major issues must be considered. The main problems that affect the system are

- How to find the best possible solution of the SWEs, and whether the positivity of the physical variables is maintained.
- Although many numerical approaches can be used to solve the system, their accuracy and efficiency are always in question.
- How to treat steady-state conditions so that a balance with accuracy is maintained.

Furthermore, while applying KFVS to solve the shallow water equations with porosity, we need to take all these points into account.

1.4 Proposed Numerical Technique

As it is not possible to find an analytical solution of the desired problem in the literature, our goal is to find a numerical scheme that is capable of solving the current model of the shallow water equations. For this purpose, in this thesis we propose a high-resolution KFVS scheme for the considered SWEs with porosity. The proposed scheme is based on an upwind-biased splitting of the flux vector. Several authors have implemented this approach to solve hyperbolic-type systems of equations. For example, Saqib Zia and Shamsul Qamar [15] applied KFVS to solve single- and two-phase shallow water flow equations. In [16], the authors used the KFVS scheme to solve a two-phase flow model with non-conservative terms. Moreover, the central scheme of Nessyahu and Tadmor [17] is applied to validate the results of the KFVS scheme. Furthermore, several test problems are presented to demonstrate the accuracy and efficiency of the proposed scheme.

1.4.1 Kinetic flux-vector splitting (KFVS) method

Flux is defined as the rate of flow of a physical quantity per unit area through a surface. To account for the well-balanced treatment of non-flat bottom topography, the shallow water model equations are used, and the scheme applied is the Kinetic Flux-Vector Splitting (KFVS) scheme [16]. In practice, due to the presence of non-flat bottom topography, applying the scheme while preserving the well-balanced property is a challenging task.

1.4.2 The Central Scheme

Annual Methodological Archive Research Review
http://amresearchreview.com/index.php/Journal/about
Volume 4, Issue 3 (2026)

Online ISSN 3007-3197
Print ISSN 3007-3189
http://amresearchreview.com/index.php/Journal/about

We use the Central scheme (NT) to solve the hyperbolic system of conservation laws. This scheme is well-organized, straightforward and efficient. This scheme is used to solve the problems in computational fluid dynamics in different fields of science and engineering, shallow flows, astrophysics, and so on. This scheme is more helpful than other schemes and this scheme did not use Riemann solvers. The first order scheme of the Lax-Friedrichs is the formation of this central scheme. It is a high-resolution scheme and free from Riemann-solver. In contrast to other schemes, this scheme does not require the problem's eigen structure, which makes this scheme more effective, straightforward and easy, and it can very well be linked to all frameworks (system) that emerge from the conservation laws. The main benefit of this scheme is that this scheme displays a large number of numerical diffusion in solutions when the time step is very small. Kurganov and Tadmor give the improved version of the central scheme for the solution of this scheme. Improving the central scheme is a technique of high resolution because it produces a small amount of dissipation. This scheme provides a universal tool for different applications because this scheme is comparatively easy and effective.

Preliminaries

In this research article, for better explanation and understanding, preliminary topics of computational fluid dynamics are included. It introduces the notions of basic and conservative fluid model formulation, hyperbolic conservation laws, weak solution and the Riemann problem.

2.1 Incompressible flows

If there is no change in the density of a fluid component during motion, a flow is said to be incompressible. The incompressible flow is an idealized case of compressible flow where pressure, temperature, and etc. differences experienced by a particle cause no change in particle density. There is really no such thing as a completely incompressible fluid. There is no change (in time) in the actual volume (and thus density) of each fluid particle in an incompressible flow. Therefore, along any given particle pathline, the density is constant (a pathline being the curve traced over time by a specific particle). Overall, however, the density of different particles may differ from each other due to the particles being at different temperatures, different compositions, or different (less likely) pressures, and so on. The flow may therefore be incompressible (the density is a constant along a pathline) and yet show variations in density (distance varies along curves that cross pathlines). For example, One sees this in stratified currents. As a particular case, if all the fluid particles in an incompressible flow have the same density, then the density is constant everywhere in the flow domain and at all times, and the flow is said to be homochoric. Liquids are

Annual Methodological Archive Research Review
http://amresearchreview.com/index.php/Journal/about
Volume 4, Issue 3 (2026)

Online ISSN 3007-3197 Print ISSN 3007-3189 http://amresearchreview.com/index.php/Journal/about

generally incompressible; water is a good example.

2.2 Conservation Laws (CL):

Conservation laws are mathematical statements that explain the movement of fluid properties that need to be conserved. This notion is fulfilled by considering fluid enclosed in certain fixed arbitrary volumes V. The net change in the conserved quantity is zero due to the fluid flow in a given time interval across S the surface of this same volume. In general, a vector of conserved variables, depending on the space coordinates and time $(x,t) = (x,y,z,t)$, is represented as

$$\mathbf{w}(\mathbf{x}\ ,\mathrm{t}) = (\mathrm{w}_1(\mathbf{x},\mathrm{t}),\mathrm{w}_2(\mathbf{x},\mathrm{t}),\dots,\mathrm{w}_m(\mathbf{x},\mathrm{t}))^T \tag{2.1}$$

where m refers to the number of vector components. The associated vector for the flux function is given by

$$\mathbf{f}(\mathbf{w})\& = \big(f_1(\mathbf{w}),f_2(\mathbf{w}),\dots,f_m(\mathbf{w})\big)^T. \tag{2.2}$$

The flow of arbitrary volume V over the surface S within the time interval $[t_0, t_0+dt]$ yields

$$\iiint_v [\mathbf{w}(\mathrm{x},\mathrm{t}_0+\mathrm{dt})-\mathbf{w}(\mathrm{x},\mathrm{t}_0)]dv + \int_{\mathrm{t}_0}^{t_0+dt}\iint_S \boldsymbol{f}(\boldsymbol{w}(x,t))\cdot \mathrm{dS}\ \mathrm{dt} = 0. \tag{2.3}$$

In the above equation, the first volume integral of the variables is taken w_i, $i = 1,\dots,m$, the second integral reflects fluxes across the S surface within the time interval of $[t_0, t_0+dt]$ at the initial and final times. The application of the fundamental calculus theorem to the first integral and the theorem of divergence to the second integral give the following expression

$$\int_{\mathrm{t}_0}^{t_0+dt}\iiint_v [\frac{\partial\ \mathrm{w}}{\partial \mathrm{t}} + \nabla.\mathrm{f}(\mathrm{w})]dv\,dt = 0. \tag{2.4}$$

Since the volume is randomly chosen, we obtain the conservation laws of the form

$$\frac{\partial\ \mathrm{w}}{\partial \mathrm{t}} + \nabla.\mathrm{f}(\mathrm{w}) \ = \ 0. \tag{2.5}$$

2.3 Hyperbolic Conservation Laws:

We deal with the hyperbolic systems of PDEs in this work. In the 1-D case, Eq. (2.5) can be expressed as

Annual Methodological Archive Research Review
http://amresearchreview.com/index.php/Journal/about
Volume 4, Issue 3 (2026)

Online ISSN 3007-3197
Print ISSN 3007-3189
http://amresearchreview.com/index.php/Journal/about

$$\frac{\partial \mathbf{w}}{\partial t} + \frac{\partial \mathbf{f}(\mathbf{w})}{\partial x} = \mathbf{0}, \tag{2.6}$$

with $\mathbf{w} = (w_1, \cdots, w_m)^T$ and $\mathbf{f} = \big(f_1(\mathbf{w}), \cdots, f_m(\mathbf{w})\big)^T$. The chain rule $\mathbf{f}'(\mathbf{w}) = \frac{\partial \mathbf{f}(\mathbf{w})}{\partial \mathbf{w}}$ allows us to reduce the system into quasi-linear form which reads as

$$\frac{\partial \mathbf{w}}{\partial \mathrm{t}} + \mathbf{f}'(\mathbf{w})\frac{\partial \mathbf{w}}{\partial \mathrm{x}} = \mathbf{0}. \tag{2.7}$$

The flux function of the Jacobian matrix are written as

$$\mathrm{A}(\mathbf{w}) = \mathbf{f}'(\mathbf{w}) = \left(\frac{\partial}{\partial \mathrm{w}_1}, \cdots, \frac{\partial}{\partial \mathrm{w}_\mathrm{m}}\right)^{\mathrm{T}} \cdot \big(f_1(\boldsymbol{w}), \cdots, f_m(\boldsymbol{w})\big). \tag{2.8}$$

The eigenvalues $\lambda_i,\ i = 1,2,\cdots,m$, of matrix A are obtained by using the relation

$$|A - \lambda I| = \det(A - \lambda I) = 0. \tag{2.9}$$

Here, I represents the $m \times m$ identity matrix. If A has m real eigenvalues $\lambda_1, \lambda_2, \cdots, \lambda_m$ with a corresponding m right eigenvectors $r_1, r_2, \cdots, r_m$ which are linearly independent then this system is called hyperbolic at a point (x, t). If all eigenvalues λ_i are distinct, system is called strictly hyperbolic.

2.4 The Riemann Problem:

The problem given the particular name as Riemann problem is basically after the name of the Bernhard Riemann, this is an initial value problem which is formed by the conservation equation involving the piecewise constant initial data and also it has a single discontinuity in the domain. In this work, the solution to Riemann's problems of SWEs equations with porosity is investigated. The Reimann problem is stated as; An initial discontinuity at $X = X_0$ separated by two states left state $\mathbf{w}^L$ and right state $\mathbf{w}^R$ with the condition $w_i^L \neq w_i^R$. The Study of a general Riemann problem allows one to analyze the behavior of weak solutions.

2.5 Weak Solution of Conservation Laws:

Conservation laws are required in integral formulation to explain fluid dynamics associated with discontinuous profiles. The solution that has been obtained is called the weak solution. Consider the one-dimensional hyperbolic system in $Eq.(2.6)$. On integrating this equation over finite volume ΔV_i having surface area S_i within domain $x_{i-1/2} \leq x \leq x_{i+1/2}$, we get

$$\int_{\Delta V_i} \left(\frac{\partial \mathbf{w}}{\partial t} + \frac{\partial \mathbf{f}(\mathbf{w})}{\partial x}\right) dV = \mathbf{0}. \tag{2.10}$$

By applying Gauss Theorem, we have

Annual Methodological Archive Research Review
http://amresearchreview.com/index.php/Journal/about
Volume 4, Issue 3 (2026)

Online ISSN 3007-3197 Print ISSN 3007-3189 http://amresearchreview.com/index.php/Journal/about

$$\int_{\Delta V_i} \frac{\partial \mathbf{f}(\mathbf{w})}{\partial x} dV = \oint_{S_i} \mathbf{f}(\mathbf{w}) \cdot dS. \quad (2.11)$$

In above equation S_i represents surface enclosing the volume ΔV_i. Thus, we obtain

$$\frac{d}{dt} \int_{\Delta V_i} \mathbf{w}\, dV + \oint_{S_i} \mathbf{f}(\mathbf{w}) \cdot dS = \mathbf{0}. \quad (2.12)$$

$Eq.(2.12)$ shows that the time change of $\mathbf{w}$ inΔV_i is because of the flux through the volume of surface S_i. On integrating $Eq.(2.12)$ over the time interval $t^n \leq t \leq t^{n+1}$, we get

$$\int_{t^n}^{t^n+1} \frac{d}{dt} \int_{\Delta V_i} \mathbf{w}\, dV + \int_{t^n}^{t^n+1} \oint_{S_i} \mathbf{f}(\mathbf{w}) \cdot dS dt = \mathbf{0}. \quad (2.13)$$

This form of conservation law is more fitting as it accepts the discontinuity of the vectors of the system. It should be noted that discontinuities can evolve even for smooth initial data in the solution of hyperbolic systems. Thus weak formulation of hyperbolic systems is therefore necessary in order to admit a discontinuous solution that is not possible in the case of differential formulation of the same system.

2.6 Shock waves

Shock waves occur supersonic flows where the flow velocity exceeds the (adiabatic) sound speed. In a product with shock flows across the surface of discontinuity. Another form of discontinuity is the so-called discontinuity of touch that can occur at any rate of flow. A discontinuity of contact is a layer that separates two liquids or gasses with different physical properties. Unlike a shock, there is no mass movement through a discontinuity of contact. The "shallow water equations" are identical to 2-D gas dynamic equations. But breaking water waves in gas dynamics tend to be more complicated than ordinary shock waves The TPSF models are derived in this research article. Firstly, the continuity and momentum equations are formulated. Afterwards, the models considered are subsequently derived.

The KFVS Scheme for SWEs with porosity

In this research article, we first present the model equations of the shallow water equations (SWEs) with porosity. Then, the high-resolution KFVS scheme is derived for the considered model. Moreover, to validate the results of the proposed scheme, we also solve the model using a finite volume scheme, namely the central scheme of Nessyahu and Tadmor [17]. Therefore, the derivation of the central scheme is also given in this research article.

3.1 The One-Dimensional Shallow Water Equations With Porosity

In this section, the details of the 1D model of SWEs with porosity are presented. As stated in [14], the 1D model equations are given as

Annual Methodological Archive Research Review
http://amresearchreview.com/index.php/Journal/about
Volume 4, Issue 3 (2026)

Online ISSN 3007-3197
Print ISSN 3007-3189
http://amresearchreview.com/index.php/Journal/about

$$\frac{\partial \boldsymbol{L}}{\partial t} + \frac{\partial M(\boldsymbol{L})}{\partial x} = \boldsymbol{N}(\boldsymbol{L}) \tag{3.1}$$

where $\boldsymbol{L}$ is the vector of conserved variables, $\boldsymbol{M}(\boldsymbol{L})$ is the physical flux vector and $\boldsymbol{N}(\boldsymbol{L})$ is the source term. The values of these vectors are:

$$\mathbf{L} = (\phi h,\ \phi hu,\ \phi)^T,\ \boldsymbol{M}(\boldsymbol{L}) = \left(\phi hu,\ \phi hu^2 + \frac{1}{2} g\phi h^2,\ 0\right)^T,$$
$$\boldsymbol{N}(\boldsymbol{L}) = \left(0,\ S_0 + S_f + \frac{1}{2} gh^2 \frac{\partial \phi}{\partial x},\ 0\right)^T \tag{3.2}$$

Here h is the water height, u is the velocity, φ is the porosity and g is the acceleration due to gravity. S_0 and S_f are the source terms related to the bottom slope and the friction, respectively, and are defined as

$$S_0 = -gh\phi \frac{\partial Z}{\partial x}, \qquad S_f = gh\phi \frac{u^2}{K^2 h^{4/3}} \tag{3.3}$$

where Z is the bottom height and K is the Strickler coefficient. Here, we neglect S_f.

3.2 The KFVS Method for Single-Phase Sallow Flows

To investigate the above model numerically, we propose a finite volume scheme named KFVS [16]. The scheme is based on the direct splitting of the macroscopic flux function of the system of equations. Here, we discuss only the 1D scheme for the flow model. In this scheme, the upwind bias in the numerical flux function is obtained in a straightforward manner. The moving particles travel either to the right or to the left, and the flux is split accordingly into a right-going and a left-going part.

$$M_{i+\frac{1}{2}} = M^+(L_i) + M^-(L_{i+1}) \tag{3.4}$$

where L_i is the cell-averaged vector of conserved variables inside the cell $I_i := [x_{i-1/2}, x_{i+1/2}]$ and M is the flux vector. In the proposed numerical scheme, we start with the data of the conserved variables and return the cell-averaged values of the conserved variables for the next time level in the same cell. The KFVS scheme has been widely used, for example, in the simulation of gas dynamics flows.

In statistical mechanics, the local Maxwellian distribution in the normal direction $n \in (x)$ is given by

$$m_L(t, n, u_n) = h\left(\frac{\lambda}{\pi}\right)^{\frac{1}{2}} \exp(-\lambda(v_n - u_n)^2); \qquad \lambda = \frac{1}{gh}\ .$$

here, u_n represent average fluid velocity, v_n velocity of the individual particle,

Annual Methodological Archive Research Review
http://amresearchreview.com/index.php/Journal/about
Volume 4, Issue 3 (2026)

Online ISSN 3007-3197 Print ISSN 3007-3189 http://amresearchreview.com/index.php/Journal/about

normalized factor is defined by λ due to the moment of the particles the flow of any material is carried out. The moving particle are splits into two group by the distribution function m_l. When the velocity is v_n greater then zero, Moreover which is greater and when the velocity is u_n less then zero velocity is negative.

$$(v^0)_n = 1 = \int_{-\infty}^{\infty} \left(\frac{\lambda}{\pi}\right)^{\frac{1}{2}} e^{-\lambda(v_n-u_n)^2}\, dv_n,$$

$$(v^1)_n = u = \int_{-\infty}^{\infty} v_n \left(\frac{\lambda}{\pi}\right)^{\frac{1}{2}} e^{-\lambda(v_n-u_n)^2}\, dv_n.$$

Both equations show that two fluxes are sufficient to split the flux.

$$(v^0)_+n = \int_{0}^{\infty} \left(\frac{\lambda}{\pi}\right)^{\frac{1}{2}} e^{-\lambda(v_n-u_n)^2} dv_n = \frac{1}{2}\,\mathrm{erfc}\left(-\sqrt{\lambda}\,u_n\right) \tag{3.5}$$

$$(v^0)_-n = \int_{-\infty}^{0} \left(\frac{\lambda}{\pi}\right)^{\frac{1}{2}} e^{-\lambda(v_n-u_n)^2} dv_n = \frac{1}{2}\,\mathrm{erfc}\left(\sqrt{\lambda}\,u_n\right) \tag{3.6}$$

also,

$$(v^1)_+n = \int_{0}^{\infty} v_n \left(\frac{\lambda}{\pi}\right)^{\frac{1}{2}} e^{-\lambda(v_n-u_n)^2} dv_n = u_n(v^0)_+n + \frac{e^{-\lambda u^2 n}}{2\sqrt{\pi\lambda}}\ , \tag{3.7}$$

$$(v^1)_-n = \int_{-\infty}^{0} v_n \left(\frac{\lambda}{\pi}\right)^{\frac{1}{2}} e^{-\lambda(v_n-u_n)^2} dv_n = u_n(v^0)_n^- - \frac{e^{-\lambda u^2 n}}{2\sqrt{\pi\lambda}} \tag{3.8}$$

The complementary error function is defined as

$$\mathrm{erfc}(x) = \frac{2}{\sqrt{\pi}} \int_{x}^{\infty} e^{-t^2}\, dt \tag{3.9}$$

First, we divide the domain into a number of cells; the finer the discretization, the smaller the possible error. Consider the cells $I_i = [x_{i-1/2}, x_{i+1/2}]$ with $i = 1,2,3,\ldots,N$. The cell faces are given as $x_{i\pm1/2} = x_i \pm \Delta x/2$. We start from the cell averages W_i^n at time t^n and compute the updated cell averages W_i^{n+1}. The time step is chosen according to the eigenvalues λ_i of the system.

By splitting the above flux function, we have

$$M(L_i) = M^+(L_i) + M^-(L_{i+1}) \tag{3.10}$$

At the left and right cell interfaces, we have

Annual Methodological Archive Research Review
http://amresearchreview.com/index.php/Journal/about
Volume 4, Issue 3 (2026)

Online ISSN 3007-3197 Print ISSN 3007-3189 http://amresearchreview.com/index.php/Journal/about

$$M_{i-\frac{1}{2}} = M_{i-1}^{+} + M_{i}^{-}, \qquad M_{i+\frac{1}{2}} = M_{i}^{+} + M_{i+1}^{-}. \tag{3.11}$$

where

$$M_{i}^{\pm} = M^{\pm}(L_i) \tag{3.12}$$

which implies that

$$M^{\pm} = (v^0)_n^{\pm}\begin{pmatrix} h \\ hu \\ 0 \end{pmatrix} + (v^0)_n^{\pm}\begin{pmatrix} 0 \\ \frac{gh^2}{2} \\ 0 \end{pmatrix},$$

Integrating over the cell $C_i = [x_{i-1/2}, x_{i+1/2}]$, the upwind scheme is

$$\frac{dL_i}{dt} = -\frac{M_{i+\frac{1}{2}} - M_{i-\frac{1}{2}}}{\Delta x} \tag{3.13}$$

where L_i is the cell-averaged value.

$$L_i(t) := \frac{1}{\Delta x}\int_{x_{i-\frac{1}{2}}}^{x_{i+\frac{1}{2}}} L\,(t,x)\,dx \tag{3.14}$$

The scheme is first-order accurate. To obtain better results, we replace the piecewise-constant values L_i by a piecewise-linear reconstruction:

$$L_i^L = L_i - \frac{1}{2}L_i^x; \qquad L_i^R = L_i + \frac{1}{2}L_i^x \tag{3.15}$$

Here, a parameter $1 \le \theta \le 2$ is used to compute the slopes as

$$L_i^x = MM\left\{\theta\Delta L_{i+\frac{1}{2}},\ \frac{\theta}{2}\left(\Delta L_{i+\frac{1}{2}} + \Delta L_{i-\frac{1}{2}}\right),\ \theta\Delta L_{i-\frac{1}{2}}\right\} \tag{3.16}$$

where Δ denotes the central difference and $1 \le \theta \le 2$ is a parameter; $\theta = 1$ gives the maximum dissipation and $\theta = 2$ gives the minimum dissipation.

$$\Delta L_{i+\frac{1}{2}} = L_{i+1} - L_i \tag{3.17}$$

For non-linear limiter, we have MM,

$$MM\{x_1, x_2, \ldots\} = \begin{cases} \min\{x_i\} & \text{if } x_i > 0 \quad \forall i, \\ \max\{x_i\} & \text{if } x_i < 0 \quad \forall i, \\ 0 & \text{otherwise} \end{cases} \tag{3.18}$$

Using the above reconstruction, a semi-discrete high-resolution kinetic solver is obtained as

$$\frac{dw_i}{dt} = -\frac{M_{i+\frac{1}{2}}(L_{i+1}^L, L_i^R) - M_{i-\frac{1}{2}}(L_i^L, L_{i-1}^R)}{\Delta x} \tag{3.19}$$

Annual Methodological Archive Research Review
http://amresearchreview.com/index.php/Journal/about
Volume 4, Issue 3 (2026)

Online ISSN 3007-3197
Print ISSN 3007-3189
http://amresearchreview.com/index.php/Journal/about

This implies:

$$M_{i+\frac{1}{2}}(L_{i+1}^{L}, L_{i}^{R}) = M_{i}^{+}(L_{i}^{R}) + M_{i+1}^{-}(L_{i+1}^{L}) \tag{3.20}$$

To obtain second-order accuracy in time, the second-order TVD Runge–Kutta method is used:

$$L^{(1)} = L^{(n)} + \Delta t\, \mathcal{L}\left(L^{(n)}\right) \tag{3.21}$$

$$L^{(n+1)} = \frac{1}{2}\left(L^{(n)} + L^{(1)} + \Delta t\, \mathcal{L}\left(L^{(1)}\right)\right), \tag{3.22}$$

where $\Delta t = t^{n+1} - t^{n}$ is the time step, which is chosen as:

$$\Delta t = \frac{\Delta x}{2 \max\limits_{1 \le i \le N} |\sigma_i|}. \tag{3.23}$$

and σ denotes the maximum eigenvalue of the system.

Now we find the source term. On careful observation, we see that the source term has only a single non-zero component. Using KFVS, it can be approximated as

$$\begin{aligned} \int_{x_{i-\frac{1}{2}}}^{x_{i+\frac{1}{2}}} N\,(L)(t,x)\, dx &= \int_{x_{i-\frac{1}{2}}}^{x_{i+\frac{1}{2}}} -g\phi h_i (z)_x\, dx \\ &= g\phi h_i \left[(z)_{i+\frac{1}{2}} - (z)_{i-\frac{1}{2}}\right] \end{aligned} \tag{3.24}$$

where φ and g are constants and $N_{i\pm 1/2}$ are the source term fluxes at the cell I_i. The source flux term is defined as $N_{i+1/2} - N_{i-1/2}$. Hence, the semi-discrete scheme is

$$\frac{dL_i}{dt} = -\frac{M_{i+\frac{1}{2}} - M_{i-\frac{1}{2}}}{\Delta x} + \frac{1}{\Delta x}\left(N_{i+\frac{1}{2}} - N_{i-\frac{1}{2}}\right). \tag{3.25}$$

Our scheme is first-order accurate. For better results, the cell-averaged variables L_i must be adjusted by interpolation. A second-order accurate MUSCL-type reconstruction is used, in which a piecewise-linear slope vector L^x is selected in the x-direction. The boundary values are given as:

$$L_i^{left} = L_i - \frac{1}{2}L_i^x, \qquad L_i^{right} = L_i + \frac{1}{2}L_i^x. \tag{3.26}$$

To compute the slopes of the discrete derivatives, a parameter $1 \le \theta \le 2$ is used, such that

$$L_i^x = \text{MinMod}\left\{\theta \Delta L_{i+\frac{1}{2}},\ \frac{\theta}{2}\left(\Delta L_{i+\frac{1}{2}} + \Delta L_{i-\frac{1}{2}}\right),\ \theta \Delta L_{i-\frac{1}{2}}\right\} \tag{3.27}$$

The central difference is denoted by:

Annual Methodological Archive Research Review
http://amresearchreview.com/index.php/Journal/about
Volume 4, Issue 3 (2026)

Online ISSN 3007-3197 Print ISSN 3007-3189 http://amresearchreview.com/index.php/Journal/about

$$\Delta L_{i+\frac{1}{2}} = L_{i+1} - L_i \tag{3.28}$$

For the non-linear limiter, we have MM,

$$MM\{x_1, x_2, \ldots\} = \begin{cases} \min\{x_i\} & \text{if } x_i > 0 \quad \forall i, \\ \max\{x_i\} & \text{if } x_i < 0 \quad \forall i, \\ 0 & \text{otherwise} \end{cases} \tag{3.29}$$

A high-resolution semi-discrete kinetic solver is:

$$\frac{dL_i}{dt} = -\frac{F_{i+\frac{1}{2}}\left(L_{i+1}^{left}, L_i^{right}\right) - F_{i-\frac{1}{2}}\left(L_i^{left}, L_{i-1}^{right}\right)}{\Delta x} + \frac{N_{i+\frac{1}{2}}\left(L_{i+1}^{left}, L_i^{right}\right) - N_{i-\frac{1}{2}}\left(L_i^{left}, L_{i-1}^{right}\right)}{\Delta x} \tag{3.30}$$

The second-order TVD Runge–Kutta scheme is used to obtain second-order accuracy in time for the above equation. Its updated form is given as:

$$L^{(1)} = L^{(n)} + \Delta t\, \mathcal{L}\left(L^{(n)}\right), \qquad L^{(n+1)} = \frac{1}{2}\left(L^{(n)} + L^{(1)} + \Delta t\, \mathcal{L}\left(L^{(1)}\right)\right) \tag{3.31}$$

The above equations give the solution at the previous time level and at the next time level.

3.3 One-dimensional central (NT) scheme

Consider the one-dimensional (1D) system described by the above equations. For this system, the central scheme of [17] is used. The predictor step is defined as:

$$\boldsymbol{L}_i^{n+1/2} = \boldsymbol{L}_i^n - \frac{\lambda}{2}\boldsymbol{M}^x(\boldsymbol{L}_i), \tag{3.32}$$

and the corrector step is given as:

$$\boldsymbol{L}_{i+1/2}^{n+1} = \frac{1}{2}(\boldsymbol{L}_i^n + \boldsymbol{L}_{i+1}^n) + \frac{1}{8}(\boldsymbol{L}_i^x + \boldsymbol{L}_{i+1}^x) + \lambda\left[\boldsymbol{M}\left(\boldsymbol{L}_i^{n+1/2}\right) - \boldsymbol{M}\left(\boldsymbol{L}_{i+1}^{n+1/2}\right)\right] + \Delta t\, M_i^{n+1/2}, \tag{3.33}$$

where, for the model equations in $Eq.(3.1)$, $\boldsymbol{M}_i^{n+1/2}$ is given by

$$M_i^{n+\frac{1}{2}} = \begin{pmatrix} 0 \\ -\frac{gh}{2}[(\phi)_i + (\phi)_{i+1}][(Z)_{i+1} - (Z)_i] + \frac{gh^2}{2}[(\phi)_{i+1} + (\phi)_i] \\ 0 \end{pmatrix}. \tag{3.34}$$

In $Eqs.(3.32)$ and $(3.33), \lambda = \Delta t/\Delta x$ and $\boldsymbol{L}_i^n$ is the cell-averaged value of $\boldsymbol{L}(t,x)$ at time $t = t^n, \boldsymbol{M}_i^x$ and $\boldsymbol{L}_i^x$ are approximations of the derivatives of $\boldsymbol{M}_i$ and $\boldsymbol{L}_i$,

Annual Methodological Archive Research Review
http://amresearchreview.com/index.php/Journal/about
Volume 4, Issue 3 (2026)

Online ISSN 3007-3197
Print ISSN 3007-3189
http://amresearchreview.com/index.php/Journal/about

respectively. These slopes can be approximated using limiters, such as the limiter (MM) defined previously. Moreover,

$$\frac{1}{\Delta x}\boldsymbol{M}^{x}(\boldsymbol{L}_i) = \frac{\partial}{\partial x}\boldsymbol{M}\big(\boldsymbol{L}(t, x = x_i)\big) + O((\Delta x)^2), \tag{3.35}$$

which represents the change in the slope (derivative) of $\boldsymbol{M}\big(\boldsymbol{L}(t, x = x_i)\big)$. To study the derivation of the central scheme further, one should be familiar with the aspects discussed above. The time step is chosen as $\Delta t \leq \frac{\Delta x}{2\max_i|\lambda_i|}$,[17], where λ_i are the eigenvalues of the Jacobian matrix. Several techniques can be used to solve hyperbolic systems of equations; the most frequently used methods are the central scheme and KFVS, as they give solutions of high accuracy in a short time. Over the past few years, a lot of work has been done to improve the accuracy of these schemes, which have mostly been used for fluid problems. The main issue when using these schemes is handling the occurrence of shocks. To overcome this deficiency, we may use half-time-step or full-time-step level discrete schemes, cell averaging, etc. Conservation laws in fully discrete form can be obtained by integration. In general, KFVS gives better results than the central scheme on the same grid points because of its better accuracy, although its implementation is not easy.

Case Studies

This research article deals with numerical test cases to check the correctness and validity of the proposed scheme. In total, four 1D problems are discussed, and the results of the two schemes, the KFVS scheme [16] and the central scheme [17], are compared.

Test Problem 1:

This is a well-known problem in the literature, called the dam-break problem. Here, we take $\varphi = 1$. As the porosity is constant, the solution resembles that of a Riemann problem with a source term. The initial discontinuity is at $x = 6$. The initial data of the problem are

$$\phi_r = 1 = \phi_l, \quad h_r = 1,\ h_l = 5, \quad u_r = 0 = u_l, \quad Z_r = 0,\ Z_l = 1.$$

The exact solution is given in [14,18,19]; the reference solution is computed at $t = 0.4s$. The numerical solution comprises a rarefaction wave, a travelling shock wave and a non-linear discontinuity at the bed step. These results are shown in $Figures$4.1 and 4.2. It is clear from the figures that the KFVS scheme captures all the waves accurately.

Annual Methodological Archive Research Review
http://amresearchreview.com/index.php/Journal/about
Volume 4, Issue 3 (2026)

Online ISSN 3007-3197 Print ISSN 3007-3189 http://amresearchreview.com/index.php/Journal/about

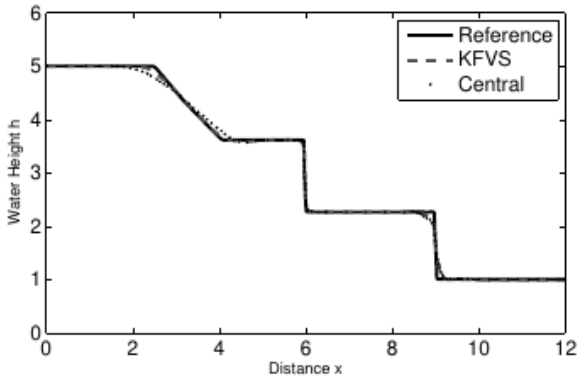

Figure 4.1: Water height at $t = 0.4$ with 200 cells is computed with constant porosity for dam-break.

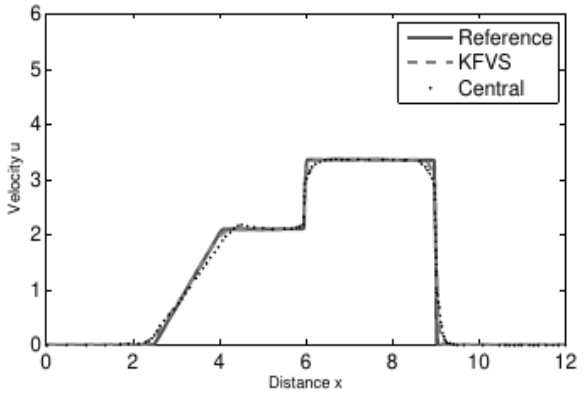

Figure 4.2: Water velocity at $t = 0.4$ with 200 cells is computed with constant porosity for dam-break.

Test Problem 2:

This test problem is included to verify that the KFVS scheme is able to maintain a stable solution [14,20]. Here, the length of the channel is $30m$ and the porosity φ is given as

$$\phi = \begin{cases} 1.0 - 0.1\cos^2\big(0.314(x-1.5)\big), & \text{if } |x-15| \le 5, \\ 1.0, & \text{otherwise.} \end{cases} \quad (4.1)$$

Moreover, the bottom topography is of the following form

$$Z = \begin{cases} 0.2\cos^2\big(0.314(x-1.5)\big), & \text{if } |x-15| \le 5, \\ 1.0, & \text{otherwise.} \end{cases} \quad (4.2)$$

Furthermore, $Z + h = 1.00m$ and $u = 0m/s$. The results are simulated with 100 grid points and the final time is $t = 500s$. *Figure*. 4.3 presents the free surface elevation, while *Figure*. 4.4 shows the discharge. A satisfactory agreement between

Annual Methodological Archive Research Review
http://amresearchreview.com/index.php/Journal/about
Volume 4, Issue 3 (2026)

Online ISSN 3007-3197
Print ISSN 3007-3189
http://amresearchreview.com/index.php/Journal/about

the results of the two schemes is observed. It can also be seen that the KFVS scheme preserves the steady-state solution.

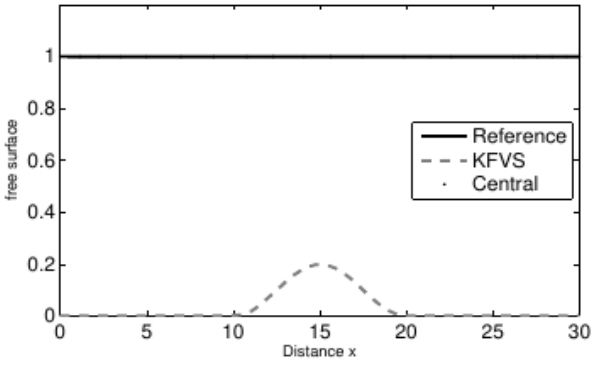

*Figure*4.3: Free surface at time $t = 500s$ for the lake at rest.

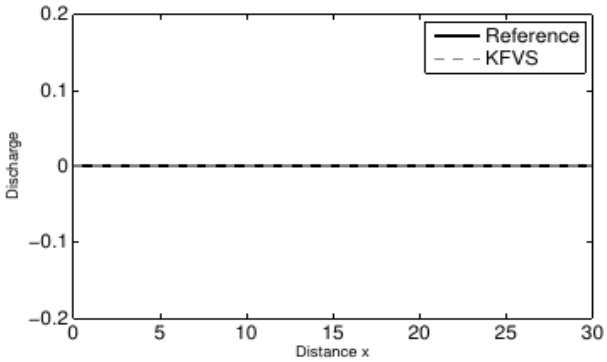

Figure 4.4: Water discharge at time $t = 500s$ for the lake at rest.

Test Problem 3:

This is also a 1D dam-break-like problem that includes a discontinuous porosity in a rectangular channel; it has also been discussed by the authors of [5,10,11,14]. The channel length is $100m$ and the initial discontinuity is placed at $x = 50m$. The initial data are given as

$\phi_l = 1.0, \quad \phi_r = 0.5, 0.1, \quad h_r = 1, \quad h_l = 10, \quad Z_l = 0 = Z_r, \quad u_l = 0 = u_r.$

The final time is $t = 3s$ for both schemes. The solution contains a rarefaction wave, a stationary discontinuity, a constant state and a shock wave. These results are shown in *Figures* 4.5 and 4.6. It can be seen from the results that the suggested schemes capture the discontinuity and shocks accurately.

Annual Methodological Archive Research Review
http://amresearchreview.com/index.php/Journal/about
Volume 4, Issue 3 (2026)

Online ISSN 3007-3197
Print ISSN 3007-3189
http://amresearchreview.com/index.php/Journal/about

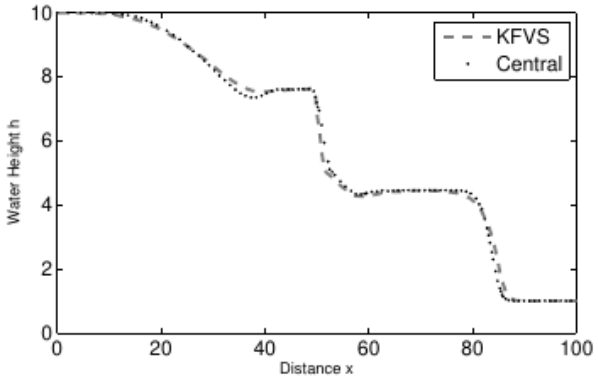

Figure 4.5: Discontinuous porosity at $t = 3s, \varphi_l = 1$ and $\varphi_r = 0.5$ for dam-break water height

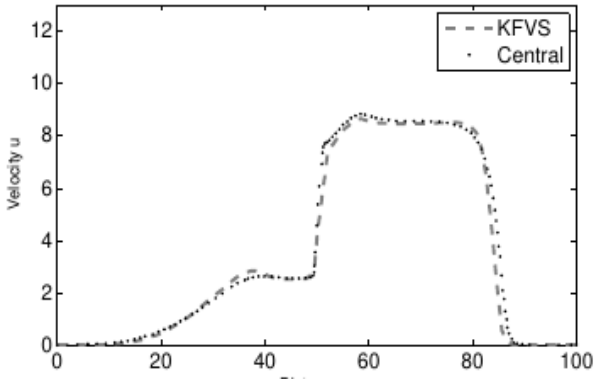

Figure 4.6: Discontinuous porosity at $t = 3s, \varphi_l = 1$ and $\varphi_r = 0.5$ for dam-break velocity

Test Problem 4:

This problem is designed to check the treatment of a dry bed. We consider a rectangular channel containing a 1D dry-bed dam break. The bottom is flat, therefore we take $Z(x) = 0$, and only the porosity is considered. Again, the channel length is $100m$ and the gate is placed at $x = 50m$. For this problem, the height and velocity are shown in *Figure* 4.9. It is clear from the figure that the proposed KFVS scheme does not require any entropy treatment for dry zones. Further, *Figure* 4.10 shows the water height above the flat bottom with discontinuous porosity, with

$$\phi_l = 1.0, \quad \phi_r = 0.5, \quad h_l = 10, \quad h_r = 1, \quad u_l = 0 = u_r, \qquad Z(x) = 0$$

The results for both schemes are simulated with 400 grid points at time $t = 3s$. The results of the KFVS scheme are better than those of the central scheme, in particular for the stationary discontinuity.

Annual Methodological Archive Research Review
http://amresearchreview.com/index.php/Journal/about
Volume 4, Issue 3 (2026)

Online ISSN 3007-3197
Print ISSN 3007-3189
http://amresearchreview.com/index.php/Journal/about

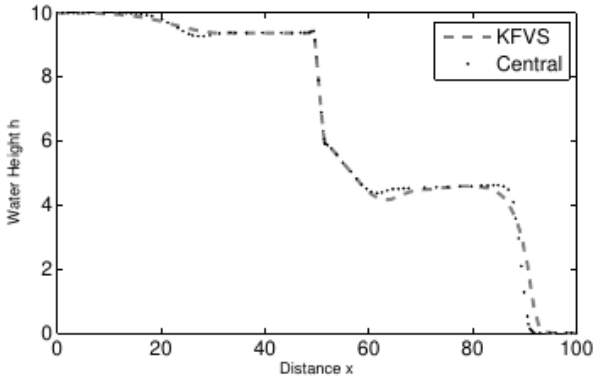

Figure 4.7: Discontinuous porosity at $t = 3s$, $\varphi_l = 1$ and $\varphi_r = 0.1$ for dam-break water height

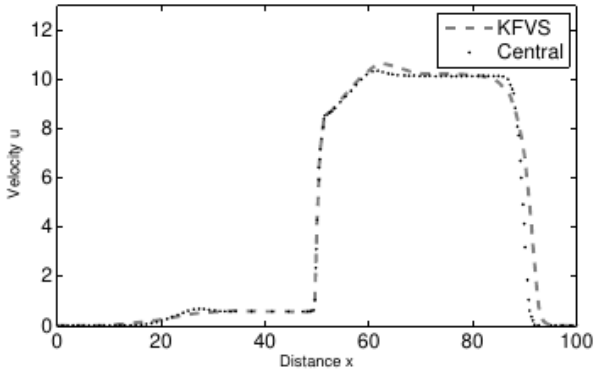

Figure 4.8: Discontinuous porosity at $t = 3s$, $\varphi_l = 1$ and $\varphi_r = 0.1$ for dam-break velocity

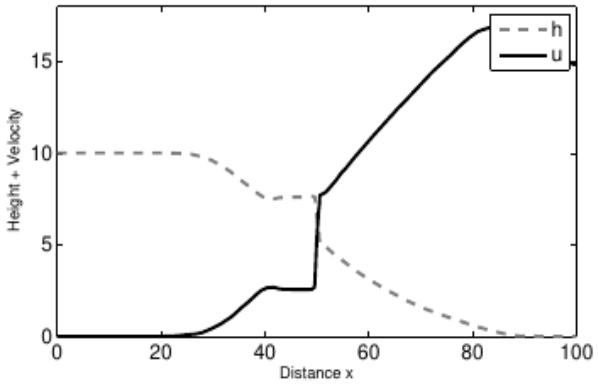

Figure 4.9: Dam-break water height with discontinuous porosity on dry bed at $t = 2s$, comparative results of wet bed height at $t = 3s$, $\varphi_l = 1$

Annual Methodological Archive Research Review
http://amresearchreview.com/index.php/Journal/about
Volume 4, Issue 3 (2026)

Online ISSN 3007-3197
Print ISSN 3007-3189
http://amresearchreview.com/index.php/Journal/about

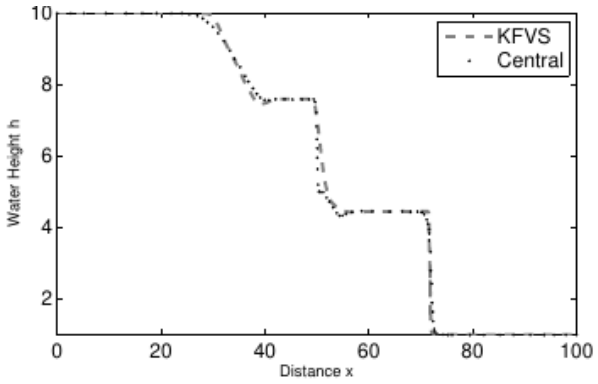

Figure 4.10: Dam-break velocity with discontinuous porosity on dry bed at $t = 2s$, comparative results of wet bed height at $t = 3$ s, $\varphi_l = 1$

Conclusions and Future Work

In this research article, we summarize the goals achieved in this work and give some recommendations for future work.

Conclusions

In this work, the one-dimensional shallow water equations with porosity, a non-conservative model used for flood simulation in urban areas, were solved numerically using a finite volume kinetic flux-vector splitting (KFVS) scheme. Since the model has no analytical solution and contains non-conservative terms, discontinuous porosity and variable bottom topography, a robust and accurate numerical method is required. The KFVS scheme was derived from the local Maxwellian distribution, which yields an upwind-biased splitting of the flux into right-going and left-going parts without the need for a Riemann solver. The source terms were discretized so that the scheme remains well balanced, and second-order accuracy was obtained using a MUSCL-type reconstruction with the minmod limiter together with a second-order TVD Runge–Kutta time integration.

To check the accuracy of the proposed scheme, the non-oscillatory central scheme of Nessyahu and Tadmor was also implemented, and the results of the two schemes were compared on four test problems. The dam-break problem over a bed step showed that the KFVS scheme captures the rarefaction wave, the travelling shock and the stationary discontinuity at the bed step accurately. The lake-at-rest problem showed that the scheme preserves the steady state, with a flat free surface and zero discharge, which confirms its well-balanced property. The dam-break problems with discontinuous porosity showed that the scheme resolves the stationary discontinuity and shock waves correctly. In the dry-bed problem, the scheme remained stable, with non-negative water height, without any entropy treatment or special handling of the

Annual Methodological Archive Research Review
http://amresearchreview.com/index.php/Journal/about
Volume 4, Issue 3 (2026)

Online ISSN 3007-3197
Print ISSN 3007-3189
http://amresearchreview.com/index.php/Journal/about

dry zones.

Overall, the two schemes were in close agreement. However, the KFVS scheme gave somewhat better resolution of sharp discontinuities, in particular at the stationary discontinuity caused by the porosity jump. It is therefore an accurate, robust and reliable tool for flow models with porosity, although its implementation is somewhat more involved than that of the central scheme.

Future Work

The present work is limited to the one-dimensional model, and the friction term was neglected. In future work, the KFVS scheme can be extended to two-dimensional shallow water equations with porosity on structured and unstructured meshes. The friction term can also be included, and the scheme can be applied to real urban flood cases with complex geometry and compared with experimental or field data. Further extensions to two-phase shallow flows with porosity, and the use of higher-order reconstructions, are other possible directions.

References

[1] A. J. C. de Saint-Venant, Theorie du mouvement non-permanent des eaux, avec application aux crues des rivieres et a l introduction des marees dans leurs lits, C. R. Acad. Sci. Paris, 73 (1871), 237-240.

[2] C. B. Vreugdenhil, (1979) Two-layer shallow water flow in two dimensions, a numerical study, J. Comput. Phys., 33, 169-184.

[3] E. B. Pitman, L. Le, (2005) A two-fluid model for avalanche and debris flows, Phil. Trans. Roy. Soc. A, 363, 1573-1601.

[4] B. F. Sanders, J. E. Schubert, H. A. Gallegos, (2008) Integral formulation of shallow water equations with anisotropic porosity for urban flood modeling, J. Hydrol., 362(1-2), 19-38.

[5] P. Finaud-Guyot, C. Delenne, J. Lhomme, V. Guinot, C. Llovel, (2010) An approximate state Riemann solver for the two-dimensional shallow water equations with porosity, Int. J. Numer. Methods Fluids, 62, 1299-1331.

[6] A. Bermudez, M. E. Vazquez, (1994) Upwind methods for hyperbolic conservation laws with source term, Computers and Fluids, 23, 1049-1071.

[7] T. Gallouet, J. M. Herard, N. Seguin, (2003) Some approximate Godunov schemes to compute shallow water equations with topography, Computers and Fluids, 32, 479-513.

[8] P. L. Roe, (1981) Approximate Riemann solvers, parameter vectors and difference schemes, J. Comput. Phys., 43, 357-372.

[9] D. Rouchette, S. Clain, (2006) Two-dimensional computation of gas flow in a porous bed characterized by a porosity jump, J. Comput. Phys., 219, 104-119.

Annual Methodological Archive Research Review
http://amresearchreview.com/index.php/Journal/about
Volume 4, Issue 3 (2026)

Online ISSN 3007-3197
Print ISSN 3007-3189
http://amresearchreview.com/index.php/Journal/about

[10] V. Guinot, S. Soares-Frazao, (2006) Flux and source term discretization in two-dimensional shallow water models with porosity on unstructured grids, Int. J. Numer. Methods Fluids, 50, 309-345.

[11] Z. L. Wang, Y. F. Geng, (2013) Two-dimensional shallow water equations with porosity and their numerical scheme on unstructured grids, Water Sci. Eng., 6(1), 91-105.

[12] K. Mohamed, (2005) Simulation numerique en volumes finis, de problemes d ecoulements multidimensionnels raides, par un schema de flux a deux pas, Dissertation, University of Paris 13.

[13] K. Mohamed, M. Seaid, M. A. Zahri, (2013) A finite volume method for scalar conservation laws with stochastic time-space dependent flux function, J. Comput. Appl. Math., 237, 614-632.

[14] K. Mohamed, (2014) A finite volume method for numerical simulation of shallow water models with porosity, Computers and Fluids, 104, 9-19.

[15] S. Zia, S. Qamar, (2014) A kinetic flux-vector splitting method for single and two-phase shallow flows, Computers and Mathematics with Applications, 67, 1271-1288.

[16] S. Qamar, M. Ahmad, (2009) A high order kinetic flux-vector splitting method for the reduced five-equation model of compressible two-fluid flows, J. Comput. Phys., 228, 9059-9078.

[17] H. Nessyahu, E. Tadmor, (1990) Non-oscillatory central differencing for hyperbolic conservation laws, J. Comput. Phys., 87, 408-448.

[18] A. Kurganov, G. Petrova, (2007) Second-order well-balanced positivity preserving central-upwind scheme for the Saint-Venant system, Commun. Math. Sci., 5, 133-160.

[19] Alcrudo, Francisco & Benkhaldoun, Fayssal. (2001). Exact solutions to the Riemann problem of the shallow water equations with a bottom step. Computers & Fluids. 30(6), 643-671.

[20] Zhili Wang Yongjun Lu Yanfen Geng. (2008). One dimensional shallow water equations with porosity and their numerical discretization scheme[J]. Chinese Journal of Theoretical and Applied Mechani, 40(5): 585-592.